

Published in final edited form as:

Nat Genet. 2012 October ; 44(10): 1142–1146. doi:10.1038/ng.2390.

Genome-wide association analyses identify three new susceptibility loci for primary angle closure glaucoma

A full list of authors and affiliations appears at the end of the article.

These authors contributed equally to this work.

Abstract

Primary angle closure glaucoma (PACG) is a major cause of blindness worldwide. We conducted a genome-wide association study including 1,854 PACG cases and 9,608 controls across 5 sample collections in Asia. Replication experiments were conducted in 1,917 PACG cases and 8,943 controls collected from a further 6 sample collections. We report significant associations at three new loci: rs11024102 in *PLEKHA7* (per-allele odds ratio (OR) = 1.22; $P = 5.33 \times 10^{-12}$), rs3753841 in *COL11A1* (per-allele OR = 1.20; $P = 9.22 \times 10^{-10}$) and rs1015213 located between *PCMTD1* and *ST18* on chromosome 8q (per-allele OR = 1.50; $P = 3.29 \times 10^{-9}$). Our findings, accumulated across these independent worldwide collections, suggest possible mechanisms explaining the pathogenesis of PACG.

Glaucoma, the leading cause of irreversible blindness worldwide¹, is characterized by progressive loss of axons in the optic nerve accompanied by visual field damage. Categorized according to the anatomy of the anterior chamber angle, two main forms of glaucoma exist: primary open-angle glaucoma (POAG) and primary angle closure glaucoma (PACG). PACG results from elevated intraocular pressure as a consequence of iris–trabecular meshwork contact in the angle of the eye, hindering aqueous outflow. Whereas POAG is the more predominant form of glaucoma in Europeans and Africans, 80% of the estimated 15 million people afflicted with PACG live in Asia². PACG is responsible for a substantial proportion of blindness in many Asian countries^{3–5}, and, in fact, it has been estimated that PACG blinds proportionately more people than POAG globally⁶.

© 2012 Nature America, Inc. All rights reserved.

Correspondence should be addressed to N. Wang (wningli@vip.163.com) or T.A. (tin11@pacific.net.sg).

³⁴These authors jointly directed this work.

AUTHOR CONTRIBUTIONS T.A., N. Wang, E.N.V. and C.-C.K. are the overall principal investigators who were jointly responsible for conception of the project, funding, study design and planning of the analysis strategy. C.Q., M.E.N., R.G., L.-J.C., T.D., K.A.-A., C.K.H., S.L., M.Z. and L.-S.A.T. are the lead coordinators for sample collection. S.A.P., L.X., H.J., C.-L.H., C.C.Y.T., R.-Y.W., P.T.K.C., D.H.S., F.T.O., N.S., E.A.O., H.-T.W., G.T., S.F., H.M., D.T.L.H., H.W., B.F., M.B., B.S., A.C.H., K.Y.L., Y.L., Y.-X.W., D.N.H., T.T.W., S.-C.L., V.K.Y.Y., A.Y., D.S.C.L. and S.A.A.-O. were the clinicians responsible for obtaining informed consent and enrolling study participants. K.S.S., W.-T.T. and X.S. performed statistical analysis. V.H.K.Y. performed gene expression analysis. C.Q., H.J., N. Wang, R.G., S.S., L.V., L.-J.C., C.K.H., M.Z. and C.-P.P. contributed to the genotyping and analysis of cases and controls for the Beijing, Chennai and Shantou samples. T.N.B.C. and C.P.S. contributed to the genotyping and analysis of the Vietnamese control group. J.-X.B. and Y.-X.Z. contributed to the genotyping and analysis of the Guangdong control group. P.J.F., L.V., T.-Y.W., C.-P.P., D.N.H., S.A.A.-O. and L.-S.A.T. are site principal investigators for their respective sample collections. S.S., C.-Y.C., V.L.R., G.K., S.K.I., T.A.S., S.M.L.T., R.L., B.K.C., Y.-F.Z., N. Waseem, K.-S.C., R.R.A., M.A.H., M.L.H., S.S.B., Y.Y.T., D.T.T., J.B.J., E.-S.T., S.-M.S. and J.L. provided intellectual input and/or contributed laboratory reagents or analysis for the project. All authors were responsible for critical revision of the manuscript. The manuscript was written by C.-C.K., E.N.V., M.E.N. and T.A.

COMPETING FINANCIAL INTERESTS The authors declare no competing financial interests.

Note: Supplementary information is available in the online version of the paper.

The pathogenesis of PACG likely involves multiple anatomical and physiological factors, and, thus, PACG shows many indications of being a complex disease with both genetic and environmental etiological factors. Epidemiological studies have suggested a genetic basis for PACG^{7–10}, and several candidate gene studies of modest sample sizes have investigated this possibility^{11–13}. However, the genetic determinants underlying individual susceptibility to PACG remain largely unknown. To identify sequence variants that confer susceptibility to PACG, we conducted a two-stage genome-wide association study (GWAS) and replication including 3,771 cases and 18,551 controls. Such staged study designs accompanied by meta-analysis have been well established^{14–18}. The discovery stage (stage 1) comprised 1,854 PACG cases and 9,608 controls recruited across 5 independent collections (Singapore, Hong Kong, India, Malaysia and Vietnam; Table 1). The replication stage (stage 2) comprised an additional 1,917 PACG cases and 8,943 controls across 6 independent collections (2 sites in China and 1 site each in Singapore, India, Saudi Arabia and the UK; Table 1).

We applied uniform quality control filters for both individual samples and SNP markers across all five PACG case-control collections for stage 1 (see Online Methods and the Supplementary Note for detailed descriptions of the sample collections). From starting numbers of 1,925 PACG cases and 9,630 controls, genotype data on 493,501 SNPs were available for 1,854 PACG cases and 9,608 controls after stringent quality control filters were applied on SNPs and samples. Within each sample collection, we ensured that each PACG case had genetically matched controls, as visualized spatially using principal-component analysis (Supplementary Fig. 1). We contrasted the genotypes between PACG cases and healthy controls via single-SNP analysis using unconditional logistic regression fitted for genotype trend effects (1-degree-of-freedom score test). As the genetic matching between cases and controls is not perfect, we adjusted the association tests with the top axes of population ancestry to remove any residual population stratification that might be present (Online Methods) within each study collection, following standard procedures^{18–23}. This was followed by random-effects meta-analysis using inverse-variance weights²⁴. We observed no evidence of genomic inflation ($\lambda_{GC} = 1.0$), thereby excluding the likelihood of significant cryptic population substructure between cases and controls. We observed association signals with genome-wide significance in *PLEKHA7* (rs11024102) on chromosome 11 (Fig. 1 and Table 2; per-allele OR = 1.27; $P = 1.43 \times 10^{-8}$) with stage 1 data alone.

A total of 15 SNPs at 12 independent loci showing evidence of association with PACG exceeding $P < 1 \times 10^{-5}$ with no evidence of heterogeneity (I^2 index = 0.0%) across the 5 sample collections in stage 1 were brought forward for replication genotyping in stage 2, which enrolled an additional 1,973 PACG cases and 9,066 controls. Similar quality control filters were applied to SNPs and samples in this stage, and 11 SNPs genotyped in a total of 1,917 PACG cases and 8,943 controls that passed quality control were brought forward for association analysis (Supplementary Table 1). Three SNP markers (rs11024102 in *PLEKHA7*, rs3753841 in *COL11A1* and rs1015213) showed significant evidence of replication in stage 2 (3.72×10^{-5} $P = 1.77 \times 10^{-4}$) and surpassed genome-wide significance in meta-analysis of all data from both stages (5.33×10^{-12} $P = 3.29 \times 10^{-9}$; Table 2, Supplementary Fig. 2 and Supplementary Table 2). Regional association analysis

for these three sequence variants clearly identified *PLEKHA7* and *COL11A1* as the likeliest candidate susceptibility genes for PACG at the associated regions in chromosomes 11 and 1, respectively, whereas rs1015213 was located in an intergenic region between *PCMTD1* and *ST18* (Fig. 2). A fourth SNP, rs3788317, in *TXNRD2* showed nominal evidence of replication in stage 2 but did not reach genome-wide significance (Supplementary Table 1). Imputation analysis of stage 1 study collections using the most recent 1000 Genomes Project Asian reference panel revealed the association of multiple SNP markers, corroborating the genotyped SNPs with the most significant association at *PLEKHA7* and *COL11A1*. Because of the rarity of rs1015213 in many Asian populations, imputation at this locus was less successful. We did not observe additional evidence of association with imputed SNPs over and above that already seen with directly genotyped SNP markers (Fig. 2). Conditional logistic regression did not reveal secondary signals of association at each of the three loci associated with genome-wide significance, suggesting that the reported most significant SNPs largely account for the observed disease associations (Supplementary Tables 3–5). Of note, no evidence of association was observed at loci previously reported to be associated with POAG^{25–27} (Supplementary Table 6). As there is a paucity of information on the identified candidate genes in the eye, we also examined the expression of *PLEKHA7*, *COL11A1*, *PCMTD1* and *ST18* in several eye tissues. We note expression of *PLEKHA7*, *COL11A1* and *PCMTD1* in tissues that form the iridocorneal angle, such as the cornea, iris and trabecular meshwork. In contrast, the expression profile of *ST18* was more limited. Although strongly expressed in the lens and cornea, *ST18* was not expressed in the trabecular meshwork or iris (Supplementary Fig. 3).

PLEKHA7 (NM_175058) encodes pleckstrin homology domain–containing protein 7, which is critical for the maintenance and stability of adherens junctions^{28,29}. In adult tissues, the adherens junctions maintain tissue homeostasis and, along with tight junctions, control epithelial and endothelial paracellular permeability³⁰. In the eye, tight junctions and adherens junctions have an essential role in structures of particular relevance to glaucoma, such as the ciliary body, iris, aqueous humor outflow system and choroid, by providing a barrier to fluid leakage³¹. Factors such as attenuated reduction in iris volume with pupillary dilation and exaggerated choroidal expansion have been proposed to have key roles in the spectrum of angle closure pathogenesis^{32–34}. Given the role of *PLEKHA7* in maintaining a protein complex that regulates paracellular permeability, we speculate that it may be involved in the pathophysiology of angle closure related to aberrant fluid dynamics. Recently, a GWAS on blood pressure in more than 60,000 individuals determined that SNPs within this gene were associated with systolic blood pressure³⁵, a systemic risk factor for glaucoma. The SNP associated with PACG in our study is located 80–100 kb upstream of the SNPs associated with blood pressure. We did not observe evidence of association between rs11024074 in *PLEKHA7*, the SNP reported to be strongly associated with systemic hypertension³⁵, and PACG status in our stage 1 meta-analysis ($P = 0.13$; per-allele OR = 1.11). The pairwise linkage disequilibrium (LD) between rs11024074 (SNP for systemic hypertension) and rs11024102 (SNP for PACG) was very weak ($D = 0.154$, $r^2 = 0.009$), suggesting that different genetic polymorphisms could underlie the subtly different mechanisms that control distinct phenotypes, even though the underlying gene is a common denominator^{36–38}.

COL11A1 (NM_001190709, NM_001854, NM_080629 and NM_080630) encodes one of the two α chains of type XI collagen. Pathogenic mutations in *COL11A1* cause Marshall syndrome (MIM 154780), Stickler syndrome, type 2 (STL2; MIM 604841) or Stickler-like syndrome³⁹. All are associated with ocular, orofacial, auditory and skeletal manifestations⁴⁰. Notably, one of the ocular features of these diseases is nonprogressive axial myopia, which is likely caused by an aberrant fibrillar collagen matrix in the sclera. Our data suggest that common variations in *COL11A1* are associated with PACG, and eyes predisposed to PACG are generally hyperopic, having a shorter axial length and a crowded anterior segment⁴¹. Therefore, the causal variants in *COL11A1* that predispose to PACG may alter its expression, such that there is the opposite effect to that observed in myopic eyes. *COL11A1* is also expressed in human ocular trabecular meshwork cells⁴², and this expression could be important in regulating the drainage of the aqueous humor from the eye. Therefore, the aberrant activity of the encoded gene product, albeit representing a mild alteration, could affect multiple sites within the eye of individuals with PACG.

The third locus, rs1015213 on chromosome 8q, is located within an intergenic region 120 kb upstream of *PCMTD1* (NM_052937) and 130 kb downstream of *ST18* (NM_014682). *PCMTD1* encodes protein-L-isoaspartate O-methyltransferase domain-containing protein 1, whose function remains relatively unknown. *ST18* encodes the suppression of tumorigenicity 18 protein and has been shown to be significantly downregulated in breast cancer cell lines⁴³. More recent studies have also shown it to be a mediator of apoptosis and inflammation⁴⁴. The LD block where rs1015213 is located extends into *PCMTD1* (Supplementary Fig. 4c) but not into *ST18*, suggesting that *PCMTD1* is the more likely candidate susceptibility gene for PACG at this locus. The minor allele frequency of rs1015213 was low (between 1–3%) in many of the sample collections (Supplementary Table 2), particularly in individuals of Chinese and Vietnamese descent. We are thus mindful that residual population stratification could confound the genetic association in these collections⁴⁵. We were somewhat reassured that 10 out of the 11 PACG sample collections showed the same direction of effect for rs1015213. Furthermore, the overall meta-analysis for all sample collections showed only mild heterogeneity (I^2 index = 19%), which was not statistically significant between the collections (P value for heterogeneity = 0.19), thus arguing against population stratification as the cause of the observed association. In terms of the biological consequences of all three loci associated with genome-wide significance, the lack of definitive biological verification and the absence of a clear mechanism mean that there remains some ambiguity as to the true causal gene(s) involved in PACG pathogenesis, although verification from independent studies and database searches (for example, UniGene (see URLs) and Gene Expression Omnibus (GEO) data sets⁴⁶) of the expression of *PLEKHA7* and *COL11A1* in ocular tissues lends some support to the idea that both genes have some role in PACG pathogenesis^{28,47}. We are unable to exclude the possibility that the identified sequence variants could be tagging the presence of functional variants that are exerting long-range control on distant gene targets in a position- and orientation-independent manner^{48,49}.

As is typical for GWAS replication studies that examine a limited number of SNPs, we were unable to formally test for population substructure in the stage 2 study collections. Our stage

2 replication involved averaging across separate results from 6 independent collections totaling 1,917 PACG cases and 8,943 controls. The inclusion of multiple populations provided insurance against false positive results, which could arise from possible substructure in some study collections. Notably, the replication collections showed evidence of association for the original stage 1 GWAS signals with consistent direction of effect and minimal heterogeneity. We note that, even in the UK replication sample that is the most distantly related to the other sample collections, the ORs for all three PACG-associated loci were no different from the stage 1, stage 2 or overall summary effect sizes (Supplementary Fig. 2). We did not observe any evidence of association at previously reported loci for POAG that surpassed genome-wide significance, despite sufficient statistical power to detect the previously reported effect sizes (Online Methods). This reinforces clinical and epidemiological data that indicate that PACG and POAG are distinct disease entities with different molecular signatures underlying their pathogenic mechanisms. As PACG is related to nanophthalmos⁵⁰, we also examined our stage 1 association results for all three reported nanophthalmos-associated loci that have been reported to date from genetic linkage studies (*NNO1* at 11p, *NNO2* at 11q23 and *NNO3* at 2q11-14)⁵⁰⁻⁵². Although rs11024102 in *PLEKHA7* was found within the broad *NNO1* locus that spans ~50 Mb, it was located outside of the 95% confidence interval (the interval encompassing a 1-unit drop in the logarithm of odds (LOD) score) for the locus. As the resolution for multiallelic microsatellite mapping was low, we are unable to rule out a role for *PLEKHA7* in susceptibility to nanophthalmos. We did not observe any other sequence variant with a stage 1 *P* value exceeding 1×10^{-5} for *NNO2* and *NNO3* (Supplementary Table 7).

Individual susceptibility to PACG has contributions from both genetic and nongenetic factors. In light of this, the use of five independent sample collections for the stage 1 discovery stage assists in the discovery of sequence variants showing the most consistent genetic association with PACG, independent of nongenetic factors that could be specific to ancestry group or nationality. The usefulness of fine mapping across ancestry groups, with the aim to localize association signals in advance of replication, could not be applied here because of the similar LD pattern across the five study collections comprising stage 1 (Supplementary Fig. 4). This is probably not unexpected, as they share Asian descent. In conclusion, we identified three new loci for PACG, a major blinding disease with largely unresolved causal mechanisms. Our findings provide insight into the genetic mechanisms responsible for individual susceptibility to PACG. Further elucidation of the genetic architecture of PACG may eventually allow the development of a clinically useful genetic profile for the identification, risk stratification and, thus, treatment of patients with PACG.

URLs. Illumina, <http://www.illumina.com/>; Sequenom, <http://www.sequenom.com/>; Applied Biosystems, <http://www.appliedbiosystems.com/>; UniGene, <http://www.ncbi.nlm.nih.gov/unigene/>; R, <http://www.r-project.org/>; IMPUTE 2, http://mathgen.stats.ox.ac.uk/impute/impute_v2.html; HapMap 3, <http://hapmap.org/>.

ONLINE METHODS

Subject enrolment and diagnosis with PACG

Detailed information on all PACG sample collections can be found in the Supplementary Note. All affected individuals were enrolled in the study after obtaining informed consent and ethical approval from the relevant national and regional institutional review boards for each sample collection. DNA was extracted from blood samples using standard laboratory procedures.

Genotyping

For stage 1, genome-wide genotyping was performed using the Illumina 610K Quad BeadChip, following the manufacturer's instructions (see URLs). For stage 2 (replication stage), genotyping was performed using the Sequenom MassArray platform (see URLs), with the exception of the Shantou collection, which was genotyped using TaqMan probes (Applied Biosystems; see URLs).

Statistical analysis

Stringent quality control filters were used to remove poorly performing samples and SNP markers in both the GWAS discovery (stage 1) and replication (stage 2) phases. SNPs with a call rate of 95% or minor allele frequency of less than 1% and those showing significant deviation from Hardy-Weinberg equilibrium (P value for deviation of $<1 \times 10^{-6}$) were removed from further statistical analysis. Likewise, samples with an overall genotyping success rate of less than 95% were removed from further analysis. The remaining samples were then subjected to biological relationship verification, using the principle of variability in allele sharing according to the degree of relationship. Identity-by-state (IBS) information was derived using PLINK⁵³. For those pairs of individuals who showed evidence of cryptic relatedness (possibly due to the presence of either duplicated or biologically related samples), we removed the sample with the lower call rate before performing principal-component analysis (PCA). PCA was undertaken to account for spurious associations resulting from ancestral differences of individual SNPs, and principal-component plots were constructed using the R statistical program package (see URLs). For stage 1, all cases had genetically matched controls, as visualized spatially on PCA for each sample collection (Supplementary Fig. 1). In addition, we have also performed a joint analysis whereby all stage 1 samples were pooled together and analyzed for association, with simultaneous adjustment for the top four principal components of genetic stratification. We observed no meaningful differences between the two methods of summarizing the stage 1 data (Supplementary Table 2).

For both the GWAS (stage 1) and replication (stage 2) phases, analysis of association with PACG disease status was carried out using a 1-degree-of-freedom score-based test using logistic regression. This test models for a trend-per-copy effect of the minor allele on disease risk. It has the best statistical power to detect association for complex traits across a wide range of alternative hypotheses, with the exception of those involving rare recessive variants. The threshold for significant independent replication was set at $P < 0.003$ (to control for 15 SNPs brought forward for replication) in the combined stage 2 data sets. For

stage 1 (GWAS discovery), we incorporated the top four principal components of genetic stratification into the logistic regression model while performing the analysis for association to minimize the effect of residual population stratification (the top ten principal components were evaluated, and, as the top four were statistically significant, they were used to control for population stratification). As stage 2 (replication) only tested 15 SNP markers, we were unable to adjust for population stratification for the stage 2 sample collections. All P values reported here are two tailed.

Meta-analysis was conducted using inverse-variance weights for each sample collection, which calculates an overall Z statistic, its corresponding P value and accompanying per-allele odds ratios for each SNP analyzed. Genotyping clusters were directly visualized for the 15 SNPs exceeding $P < 1 \times 10^{-5}$ and were confirmed to be of good quality before inclusion for statistical analysis. Illumina and Sequenom cluster plots are shown in Supplementary Figure 5a,b, respectively, for the SNPs surpassing the formal threshold for genome-wide significance ($P < 5 \times 10^{-8}$): rs11024012 (*PLEKHA7*), rs3753841 (*COL11A1*) and rs1015213 (chromosome 8q). The I^2 (I -squared) index was calculated to quantify the extent of heterogeneity between sample collections in the meta-analysis. $I^2 < 25\%$ reflects low heterogeneity, $25\% < I^2 < 50\%$ reflects moderate heterogeneity, and $I^2 > 50\%$ reflects high heterogeneity. Analysis of LD was performed using the R software package.

Genotype imputation

Fine-scale imputation at the three loci reaching genome-wide significance was performed using all 1,854 PACG cases and 9,608 controls that passed stage 1 quality control filters. Imputation was carried out using IMPUTE2 version 2.2.2 with Asian (ASI) population haplotypes from the 1000 Genomes Project⁵⁴ June 2011 release as the reference. For study collections of Chinese, Malay and Indian descent, a second reference panel consisting of related haplotypes from HapMap 3 release 3 and the Singapore Genome Variation Project (SVGP)⁵⁵ were also used for the imputation.

Imputed genotypes were called with an impute probability threshold of 0.9, with all other genotypes classified as missing. Additional quality control filters were applied to remove SNPs with more than 1% missingness if the SNP had a minor allele frequency below 5% in either cases or controls. For common SNPs with minor allele frequency above 5%, SNPs were filtered out if there was more than 5% missingness.

Power calculations

All statistical power calculations were performed as previously described^{37,56}. For the stage 1 discovery analysis, power calculations indicated that there was 90% power of detecting loci at $P < 1.0 \times 10^{-5}$ (the threshold for following up sequence variants in stage 2) at minor allele frequencies as low as 15% with per-allele odds ratios of 1.30.

The entire sample set of 3,771 PACG cases and 18,551 controls had 90% power to detect loci at the formal threshold for genome-wide significance ($P < 5.0 \times 10^{-8}$) at minor allele frequencies as low as 15% with per-allele odds ratios as low as 1.25, in line with the effect sizes we report in this manuscript. Supplementary Table 8a shows the formal power

calculations in the context of the final meta-analysis, and Supplementary Table 8b shows the power calculations to detect SNPs at the threshold of $P < 1 \times 10^{-5}$ in stage 1.

Gene expression analysis

The expression of the *PLEKHA7*, *COL11A1*, *PCMTD1* and *ST18* genes was assessed by semiquantitative RT-PCR, using primers selected specifically to target the mRNA and not the genomic DNA of these genes (Supplementary Table 9). All gene-specific primers therefore spanned an intron, and the PCR product sizes obtained (*PLEKHA7*, 206 bp; *COL11A1*, 242 bp; *PCMTD1*, 166 bp; *ST18*, 223 bp) confirmed the amplification of mRNA. Total RNA was extracted from a variety of ocular tissues (sclera, cornea, iris, trabecular meshwork, lens, lens capsule, retina and retinal pigment epithelium, choroid, optic nerve head and optic nerve) with TRIzol Reagent (Invitrogen) in accordance with the manufacturer's protocol. First-strand cDNA synthesis was performed with the SuperScript First-Strand Synthesis System for RT-PCR (Invitrogen) using random primers. Semiquantitative RT-PCR was performed according to the manufacturer's protocol with SYBR Green Master Mix (Invitrogen), using the gene-specific primers and equal amounts of cDNA template. The resulting PCR products were separated on a 2% agarose gel and visualized by ethidium bromide staining. The ubiquitously expressed *ACTB* gene (encoding β -actin) was used as an amplification and normalization control. All RT-PCR products were resequenced to confirm that the correct template was targeted by the primer pair selected for each gene. Semiquantitative RT-PCR was performed three times to confirm the expression results, and a representative agarose gel picture is shown.

Supplementary Material

Refer to Web version on PubMed Central for supplementary material.

Authors

Eranga N Vithana^{#1,2,3,4}, Chiea-Chuen Khor^{#1,2,3,4,5,6,34}, Chunyan Qiao^{#7}, Monisha E Nongpiur^{1,2}, Ronnie George⁸, Li-Jia Chen⁹, Tan Do¹⁰, Khaled Abu-Amero^{11,12}, Chor Kai Huang¹³, Sancy Low¹⁴, Liza-Sharmini A Tajudin¹⁵, Shamira A Perera¹, Ching-Yu Cheng^{1,2,6}, Liang Xu¹⁶, Hongyan Jia⁷, Ching-Lin Ho¹, Kar Seng Sim⁴, Ren-Yi Wu^{1,17}, Clement C Y Tham⁹, Paul T K Chew², Daniel H Su¹, Francis T Oen¹, Sripriya Sarangapani⁸, Nagaswamy Soumittra⁸, Essam A Osman¹¹, Hon-Tym Wong¹⁸, Guangxian Tang¹⁹, Sujie Fan²⁰, Hailin Meng²¹, Dao T L Huong¹⁰, Hua Wang⁷, Bo Feng⁷, Mani Baskaran¹, Balekudaru Shantha⁸, Vedam L Ramprasad⁸, Govindasamy Kumaramanickavel⁸, Sudha K Iyengar²², Alicia C How¹, Kelvin Y Lee¹, Theru A Sivakumaran²², Victor H K Yong¹, Serena M L Ting¹, Yang Li¹⁵, Ya-Xing Wang¹⁶, Wan-Ting Tay¹, Xueling Sim²³, Raghavan Lavanya¹, Belinda K Cornes¹, Ying-Feng Zheng^{1,2}, Tina T Wong¹, Seng-Chee Loon², Vernon K Y Yong¹⁸, Naushin Waseem¹⁴, Azhany Yaakub¹⁵, Kee-Seng Chia⁶, R Rand Allingham²⁴, Michael A Hauser²⁴, Dennis S C Lam⁹, Martin L Hibberd^{3,6}, Shomi S Bhattacharya¹⁴, Mingzhi Zhang¹³, Yik Ying Teo^{4,6,23}, Donald T Tan^{1,2}, Jost B Jonas²⁵, E-Shyong Tai^{6,26,27}, Seang-Mei Saw^{1,6}, Do Nhu Hon¹⁰, Saleh A Al-Obeidan¹¹, Jianjun Liu^{4,6}, Tran Nguyen Bich Chau²⁸, Cameron P Simmons^{28,29},

Jin-Xin Bei^{30,31}, Yi-Xin Zeng^{30,31,32}, Paul J Foster¹⁴, Lingam Vijaya⁸, Tien-Yin Wong^{1,2,6}, Chi-Pui Pang⁹, Ningli Wang^{#7,34}, and Tin Aung^{#1,2,34}

Affiliations

- ¹Singapore Eye Research Institute, Singapore National Eye Centre, Singapore.
- ²Department of Ophthalmology, National University Health System & National University of Singapore, Singapore.
- ³Infectious Diseases, Genome Institute of Singapore, Singapore.
- ⁴Human Genetics, Genome Institute of Singapore, Singapore.
- ⁵Department of Paediatrics, National University Health System & National University of Singapore, Singapore.
- ⁶Saw Swee Hock School of Public Health, National University of Singapore, Singapore.
- ⁷Beijing Ophthalmology & Visual Sciences Key Laboratory, Beijing Tongren Eye Center, Beijing Tongren Hospital, Capital Medical University, Beijing, China.
- ⁸Vision Research Foundation, Sankara Nethralaya, Chennai, India.
- ⁹Department of Ophthalmology & Visual Sciences, Chinese University of Hong Kong, Hong Kong, China.
- ¹⁰Vietnam National Institute of Ophthalmology, Hanoi, Vietnam.
- ¹¹Department of Ophthalmology, College of Medicine, King Saud University, Riyadh, Saudi Arabia.
- ¹²Department of Ophthalmology, College of Medicine, University of Florida, Jacksonville, Florida, USA.
- ¹³Shantou University–Chinese University of Hong Kong Joint Shantou International Eye Center, Shantou, China.
- ¹⁴National Institute for Health Research (NIHR) Biomedical Research Centre for Ophthalmology at Moorfields Eye Hospital and University College London (UCL) Institute of Ophthalmology, London, UK.
- ¹⁵Department of Ophthalmology, School of Medical Sciences, Universiti Sains Malaysia, Kota Bharu, Malaysia.
- ¹⁶Beijing Institute of Ophthalmology, Beijing Tongren Hospital, Capital Medical University, Beijing, China.
- ¹⁷Xiamen Eye Centre, Xiamen University, Xiamen, China.
- ¹⁸Department of Ophthalmology, Tan Tock Seng Hospital, Singapore.
- ¹⁹Xingtai Eye Hospital, Xingtai, China.
- ²⁰Handan Eye Hospital, Handan, China.

- ²¹Anyang Eye Hospital, Anyang, China.
- ²²Department of Epidemiology and Biostatistics, Case Western Reserve University, Cleveland, Ohio, USA.
- ²³Centre for Molecular Epidemiology, National University of Singapore, Singapore.
- ²⁴Department of Ophthalmology, Duke University Medical Center, Durham, North Carolina, USA.
- ²⁵Department of Ophthalmology, Medical Faculty Mannheim of the Ruprecht-Karls-University Heidelberg, Heidelberg, Germany.
- ²⁶Department of Medicine, National University Health System & National University of Singapore, Singapore.
- ²⁷Duke–National University of Singapore Graduate Medical School, Singapore.
- ²⁸Oxford University Clinical Research Unit, Ho Chi Minh City, Vietnam.
- ²⁹Centre for Tropical Medicine, Nuffield Department of Clinical Medicine, Oxford University, Oxford, UK.
- ³⁰State Key Laboratory of Oncology in Southern China, Guangzhou, China.
- ³¹Department of Experimental Research, Sun Yat-Sen University Cancer Centre, Guangzhou, China.
- ³²Peking Union Medical College, Chinese Academy of Medical Science, Beijing, China.

ACKNOWLEDGMENTS

The authors thank all individuals with PACG and controls who have participated in this genetic study. We thank the following for contribution of cases and controls: J. Chua, D. Goh, R. Husain, N. Amerasinghe and A. Narayanaswamy of the Singapore National Eye Centre/Singapore Eye Research Institute; L.H. Thean, C. Aquino, C. Sng and A. Tan of the National University Hospital, Singapore; B.-A. Lim and L. Yip of Tan Tock Seng Hospital, Singapore; and Y. Liang, S. Li, X. Duan, F. Wang, X. Yang, Q. Zhou and X. Yang of the Handan Eye Study, China. The authors would also like to thank C. Chakarova, P. Ostergaard, S. Jeffery, H.J. Cordell, P.T. Khaw, D.F. Garway-Heath, A.C. Viswanathan, W.-Y. Meah, S. Chen, D. Venkataraman, L.-W. Koh, X.Y. Ng, H.-B. Toh, K.-K. Heng and X.Y. Chen for administrative, technical and genotyping support. This work was supported by grants from the National Medical Research Council, Singapore (NMRC/TCR/002-SERI/2008 (R626/47/2008TCR), CSA R613/34/2008, NMRC 0796/2003 and STaR/0003/2008), the National Research Foundation of Singapore, the Biomedical Research Council, Singapore (BMRC 09/1/35/19/616 and 08/1/35/19/550), Genome Institute of Singapore Intramural funding, the Beijing Municipal Natural Science Foundation (7102036), the Key Project of the Beijing Municipal Natural Science Foundation (7081001) and the Key Project of the National Natural Science Foundation of China (81030016).

References

1. Thylefors B, Negrel AD, Pararajasegaram R, Dadzie KY. Global data on blindness. *Bull. World Health Organ.* 1995; 73:115–121. [PubMed: 7704921]
2. Quigley HA, Broman AT. The number of people with glaucoma worldwide in 2010 and 2020. *Br. J. Ophthalmol.* 2006; 90:262–267. [PubMed: 16488940]
3. Foster PJ, Johnson GJ. Glaucoma in China: how big is the problem? *Br. J. Ophthalmol.* 2001; 85:1277–1282. [PubMed: 11673287]

4. Hornby SJ, Adolph S, Gilbert CE, Dandona L, Foster A. Visual acuity in children with coloboma: clinical features and a new phenotypic classification system. *Ophthalmology*. 2000; 107:511–520. [PubMed: 10711890]
5. Dandona L, et al. Angle-closure glaucoma in an urban population in southern India. The Andhra Pradesh eye disease study. *Ophthalmology*. 2000; 107:1710–1716. [PubMed: 10964834]
6. Quigley HA, Congdon NG, Friedman DS. Glaucoma in China (and worldwide): changes in established thinking will decrease preventable blindness. *Br. J. Ophthalmol*. 2001; 85:1271–1272. [PubMed: 11673284]
7. Lowe RF. Primary angle-closure glaucoma. Inheritance and environment. *Br. J. Ophthalmol*. 1972; 56:13–20. [PubMed: 5058710]
8. Amerasinghe N, et al. The heritability and sibling risk of angle closure in Asians. *Ophthalmology*. 2011; 118:480–485. [PubMed: 21035870]
9. Congdon N, Wang F, Tielsch JM. Issues in the epidemiology and population-based screening of primary angle-closure glaucoma. *Surv. Ophthalmol*. 1992; 36:411–423. [PubMed: 1589856]
10. Wong TY, Loon SC, Saw SM. The epidemiology of age related eye diseases in Asia. *Br. J. Ophthalmol*. 2006; 90:506–511. [PubMed: 16547337]
11. Awadalla MS, Thapa SS, Burdon KP, Hewitt AW, Craig JE. The association of hepatocyte growth factor (*HGF*) gene with primary angle closure glaucoma in the Nepalese population. *Mol. Vis*. 2011; 17:2248–2254. [PubMed: 21897747]
12. Awadalla MS, Burdon KP, Kuot A, Hewitt AW, Craig JE. Matrix metalloproteinase-9 genetic variation and primary angle closure glaucoma in a Caucasian population. *Mol. Vis*. 2011; 17:1420–1424. [PubMed: 21655354]
13. Michael S, Qamar R, Akhtar F, Khan WA, Ahmed A. C677T polymorphism in the methylenetetrahydrofolate reductase gene is associated with primary closed angle glaucoma. *Mol. Vis*. 2008; 14:661–665. [PubMed: 18385801]
14. Ghousaini M, et al. Genome-wide association analysis identifies three new breast cancer susceptibility loci. *Nat. Genet*. 2012; 44:312–318. [PubMed: 22267197]
15. Thomas G, et al. A multistage genome-wide association study in breast cancer identifies two new risk alleles at 1p11.2 and 14q24.1 (*RAD51LI*). *Nat. Genet*. 2009; 41:579–584. [PubMed: 19330030]
16. Kote-Jarai Z, et al. Seven prostate cancer susceptibility loci identified by a multistage genome-wide association study. *Nat. Genet*. 2011; 43:785–791. [PubMed: 21743467]
17. Bellenguez C, et al. Genome-wide association study identifies a variant in *HDAC9* associated with large vessel ischemic stroke. *Nat. Genet*. 2012; 44:328–333. [PubMed: 22306652]
18. Kooner JS, et al. Genome-wide association study in individuals of South Asian ancestry identifies six new type 2 diabetes susceptibility loci. *Nat. Genet*. 2011; 43:984–989. [PubMed: 21874001]
19. Australia and New Zealand Multiple Sclerosis Genetics Consortium (ANZgene). Genome-wide association study identifies new multiple sclerosis susceptibility loci on chromosomes 12 and 20. *Nat. Genet*. 2009; 41:824–828. [PubMed: 19525955]
20. Reveille JD, et al. Genome-wide association study of ankylosing spondylitis identifies non-MHC susceptibility loci. *Nat. Genet*. 2010; 42:123–127. [PubMed: 20062062]
21. Khor CC, et al. Genome-wide association study identifies *FCGR2A* as a susceptibility locus for Kawasaki disease. *Nat. Genet*. 2011; 43:1241–1246. [PubMed: 22081228]
22. Höglinger GU, et al. Identification of common variants influencing risk of the tauopathy progressive supranuclear palsy. *Nat. Genet*. 2011; 43:699–705. [PubMed: 21685912]
23. Sawcer S, et al. Genetic risk and a primary role for cell-mediated immune mechanisms in multiple sclerosis. *Nature*. 2011; 476:214–219. [PubMed: 21833088]
24. Nalls MA, et al. Imputation of sequence variants for identification of genetic risks for Parkinson's disease: a meta-analysis of genome-wide association studies. *Lancet*. 2011; 377:641–649. [PubMed: 21292315]
25. Burdon KP, et al. Genome-wide association study identifies susceptibility loci for open angle glaucoma at *TMCO1* and *CDKN2B-AS1*. *Nat. Genet*. 2011; 43:574–578. [PubMed: 21532571]

26. Thorleifsson G, et al. Common variants near *CAVI* and *CAV2* are associated with primary open-angle glaucoma. *Nat. Genet.* 2010; 42:906–909. [PubMed: 20835238]
27. Wiggs JL, et al. Common variants near *CAVI* and *CAV2* are associated with primary open-angle glaucoma in Caucasians from the USA. *Hum. Mol. Genet.* 2011; 20:4707–4713. [PubMed: 21873608]
28. Pulimeno P, Bauer C, Stutz J, Citi S. PLEKHA7 is an adherens junction protein with a tissue distribution and subcellular localization distinct from ZO-1 and E-cadherin. *PLoS ONE.* 2010; 5:e12207. [PubMed: 20808826]
29. Meng W, Mushika Y, Ichii T, Takeichi M. Anchorage of microtubule minus ends to adherens junctions regulates epithelial cell-cell contacts. *Cell.* 2008; 135:948–959. [PubMed: 19041755]
30. Harris TJ, Tepass U. Adherens junctions: from molecules to morphogenesis. *Nat. Rev. Mol. Cell Biol.* 2010; 11:502–514. [PubMed: 20571587]
31. Tian B, Geiger B, Epstein DL, Kaufman PL. Cytoskeletal involvement in the regulation of aqueous humor outflow. *Invest. Ophthalmol. Vis. Sci.* 2000; 41:619–623. [PubMed: 10711672]
32. Quigley HA, et al. Iris cross-sectional area decreases with pupil dilation and its dynamic behavior is a risk factor in angle closure. *J. Glaucoma.* 2009; 18:173–179. [PubMed: 19295366]
33. Quigley HA, Friedman DS, Congdon NG. Possible mechanisms of primary angle-closure and malignant glaucoma. *J. Glaucoma.* 2003; 12:167–180. [PubMed: 12671473]
34. Aptel F, Denis P. Optical coherence tomography quantitative analysis of iris volume changes after pharmacologic mydriasis. *Ophthalmology.* 2010; 117:3–10. [PubMed: 19923002]
35. Levy D, et al. Genome-wide association study of blood pressure and hypertension. *Nat. Genet.* 2009; 41:677–687. [PubMed: 19430479]
36. Davila S, et al. Genome-wide association study identifies variants in the *CFH* region associated with host susceptibility to meningococcal disease. *Nat. Genet.* 2010; 42:772–776. [PubMed: 20694013]
37. Gharavi AG, et al. Genome-wide association study identifies susceptibility loci for IgA nephropathy. *Nat. Genet.* 2011; 43:321–327. [PubMed: 21399633]
38. Klein RJ, et al. Complement factor H polymorphism in age-related macular degeneration. *Science.* 2005; 308:385–389. [PubMed: 15761122]
39. Richards AJ, et al. A family with Stickler syndrome type 2 has a mutation in the *COL11A1* gene resulting in the substitution of glycine 97 by valine in $\alpha 1(XI)$ collagen. *Hum. Mol. Genet.* 1996; 5:1339–1343. [PubMed: 8872475]
40. Snead MP, Yates JR. Clinical and molecular genetics of Stickler syndrome. *J. Med. Genet.* 1999; 36:353–359. [PubMed: 10353778]
41. George R, et al. Ocular biometry in occludable angles and angle closure glaucoma: a population based survey. *Br. J. Ophthalmol.* 2003; 87:399–402. [PubMed: 12642298]
42. Michael I, Shmoish M, Walton DS, Levenberg S. Interactions between trabecular meshwork cells and lens epithelial cells: a possible mechanism in infantile aphakic glaucoma. *Invest. Ophthalmol. Vis. Sci.* 2008; 49:3981–3987. [PubMed: 18469193]
43. Jandrig B, et al. ST18 is a breast cancer tumor suppressor gene at human chromosome 8q11.2. *Oncogene.* 2004; 23:9295–9302. [PubMed: 15489893]
44. Yang J, Siqueira MF, Behl Y, Alikhani M, Graves DT. The transcription factor ST18 regulates proapoptotic and proinflammatory gene expression in fibroblasts. *FASEB J.* 2008; 22:3956–3967. [PubMed: 18676404]
45. Mathieson I, McVean G. Differential confounding of rare and common variants in spatially structured populations. *Nat. Genet.* 2012; 44:243–246. [PubMed: 22306651]
46. Diehn JJ, Diehn M, Marmor MF, Brown PO. Differential gene expression in anatomical compartments of the human eye. *Genome Biol.* 2005; 6:R74. [PubMed: 16168081]
47. Jun AS, et al. Microarray analysis of gene expression in human donor corneas. *Arch. Ophthalmol.* 2001; 119:1629–1634. [PubMed: 11709013]
48. Pomerantz MM, et al. The 8q24 cancer risk variant rs6983267 shows long-range interaction with *MYC* in colorectal cancer. *Nat. Genet.* 2009; 41:882–884. [PubMed: 19561607]

49. Tuupanen S, et al. The common colorectal cancer predisposition SNP rs6983267 at chromosome 8q24 confers potential to enhanced Wnt signaling. *Nat. Genet.* 2009; 41:885–890. [PubMed: 19561604]
50. Othman MI, et al. Autosomal dominant nanophthalmos (NNO1) with high hyperopia and angle-closure glaucoma maps to chromosome 11. *Am. J. Hum. Genet.* 1998; 63:1411–1418. [PubMed: 9792868]
51. Sundin OH, et al. Extreme hyperopia is the result of null mutations in *MFRP*, which encodes a Frizzled-related protein. *Proc. Natl. Acad. Sci. USA.* 2005; 102:9553–9558. [PubMed: 15976030]
52. Li H, et al. Localization of a novel gene for congenital nonsyndromic simple microphthalmia to chromosome 2q11–14. *Hum. Genet.* 2008; 122:589–593. [PubMed: 17924146]
53. Purcell S, et al. PLINK: a tool set for whole-genome association and population-based linkage analyses. *Am. J. Hum. Genet.* 2007; 81:559–575. [PubMed: 17701901]
54. 1000 Genomes Project Consortium. A map of human genome variation from population-scale sequencing. *Nature.* 2010; 467:1061–1073. [PubMed: 20981092]
55. Teo YY, et al. Singapore Genome Variation Project: a haplotype map of three Southeast Asian populations. *Genome Res.* 2009; 19:2154–2162. [PubMed: 19700652]
56. Purcell S, Cherny SS, Sham PC. Genetic Power Calculator: design of linkage and association genetic mapping studies of complex traits. *Bioinformatics.* 2003; 19:149–150. [PubMed: 12499305]

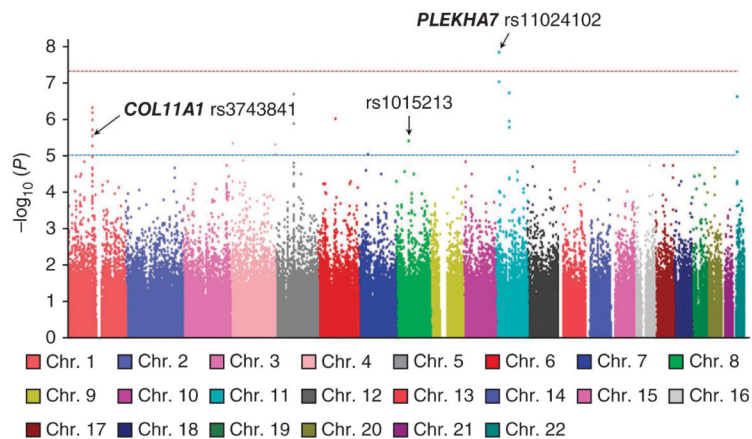
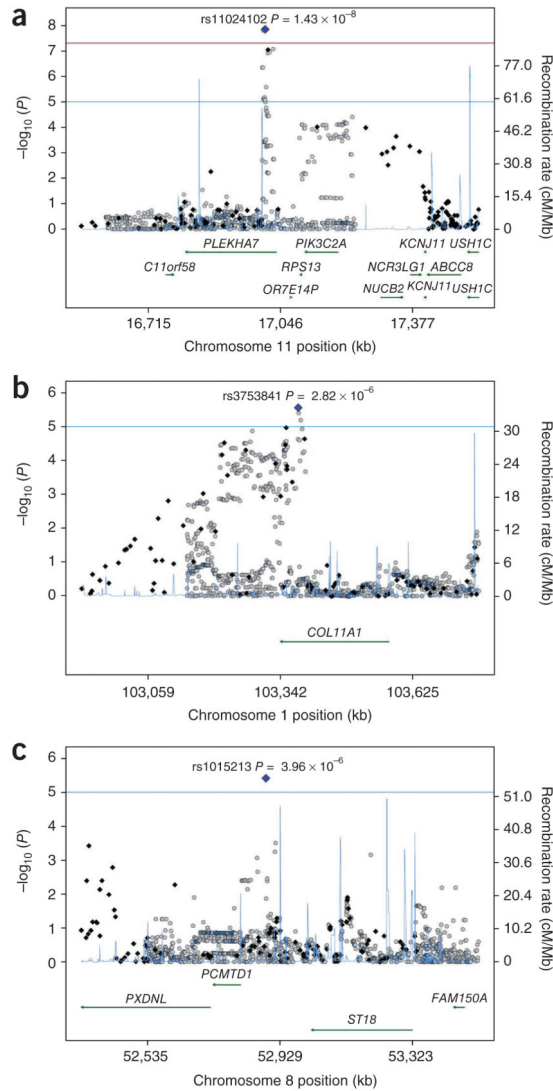


Figure 1.

Manhattan plot of all stage 1 data for 1,854 PACG cases and 9,609 controls. SNP markers are plotted according to chromosomal location on the x axis, with the $-\log_{10} P$ values on the y axis derived from the 1-degree-of-freedom score test. The blue horizontal dashed line ($P < 1 \times 10^{-5}$) denotes the threshold for bringing genetic loci forward for further testing in stage 2. The red horizontal dashed line ($P < 5 \times 10^{-8}$) shows the formal threshold for genome-wide significance.

**Figure 2.**

Regional association and recombination rate plots for stage 1 data. (a–c) Data are shown for the *PLEKHA7* locus around rs11024102 (a), the *COL11A1* locus around rs3753841 (b) and the chromosome 8q locus around rs1015213 (c). Data shown are for both imputed (gray circles) and directly genotyped (black diamonds) SNPs. The genotyped SNP with the most significant association is denoted with a blue diamond. The left y axis represents $-\log_{10} P$ values for association with PACG in stage 1, the right y axis represents the recombination rate, and the x axis represents base-pair positions along the chromosome (human genome Build 37). The blue and red horizontal lines denote $P = 1 \times 10^{-5}$ and $P = 5 \times 10^{-8}$, respectively.

Table 1
Sample collections of PACG cases and controls for stages 1 (GWAS discovery) and 2 (replication)

Collection	PACG cases (N)	Controls (N)
Stage 1		
Singapore (Chinese)	984	943
Hong Kong (Chinese)	297	1,044 ^a
Malaysia (Malay)	83	3,065 ^a
India (Indian)	337	2,538 ^a
Vietnam (Vietnamese)	153	2,018 ^a
All stage 1	1,854	9,608
Stage 2		
Singapore (Chinese)	309	1,479
Beijing (Chinese)	992	1,672
Saudi (Middle Eastern descent)	165	175
UK (European descent)	127	4,703 ^a
India (Indian)	80	309
Shantou (Chinese)	244	605
All stage 2	1,917	8,943
All samples	3,771	18,551

^aControl collections represent population-based controls who were not examined for PACG disease status.

Table 2

Genome-wide significant associations from the GWAS of PACG

Chromosome	SNP	Gene	GWAS (stage 1)			Replication (stage 2)			All data (stages 1 and 2)		
			A1	OR	P	OR	P	OR	P	P_{het}	I^2 (%)
11	rs11024102	PLEKHA7	G	1.27	1.43×10^{-8}	1.18	3.72×10^{-5}	1.22	5.33×10^{-12}	0.64	0
1	rs3753841	COL11A1	G	1.22	2.82×10^{-6}	1.18	6.62×10^{-5}	1.20	9.22×10^{-10}	0.59	0
8	rs1015213	PCMTD1-ST18	A	1.56	3.90×10^{-6}	1.44	1.77×10^{-4}	1.50	3.29×10^{-9}	0.19	19.0

A1, effect allele; OR, per-allele odds ratio of the effect allele; P, P value for association; P_{het} , P value for heterogeneity between collections; I^2 , I-squared index quantifying heterogeneity (Online Methods).